Received: 12 May 2022 | Revised: 25 July 2022 | Accepted: 24 August 2022

DOI: 10.4218/etrij.2022-0184

ORIGINAL ARTICLE

ETRI Journal WILEY

# Optimum solar energy harvesting system using artificial intelligence

**Sunardi Sangsang Sasmowiyono** | **Abdul Fadlil** | **Arsyad Cahya Subrata**

Department of Electrical Engineering, Universitas Ahmad Dahlan, Yogyakarta, Indonesia

**Correspondence**
Sunardi Sangsang Sasmowiyono, Department of Electrical Engineering, Universitas Ahmad Dahlan, Yogyakarta, Indonesia.
Email: sunardi@mti.uad.ac.id

**Abstract**

Renewable energy is promoted massively to overcome problems that fossil fuel power plants generate. One popular renewable energy type that offers easy installation is a photovoltaic (PV) system. However, the energy harvested through a PV system is not optimal because influenced by exposure to solar irradiance in the PV module, which is constantly changing caused by weather. The maximum power point tracking (MPPT) technique was developed to maximize the energy potential harvested from the PV system. This paper presents the MPPT technique, which is operated on a new high-gain voltage DC/DC converter that has never been tested before for the MPPT technique in PV systems. Fuzzy logic (FL) was used to operate the MPPT technique on the converter. Conventional and adaptive perturb and observe (P&O) techniques based on variables step size were also used to operate the MPPT. The performance generated by the FL algorithm outperformed conventional and variable step-size P&O. It is evident that the oscillation caused by the FL algorithm is more petite than variables step-size and conventional P&O. Furthermore, FL's tracking speed algorithm for tracking MPP is twice as fast as conventional P&O.

**KEYWORDS**

artificial intelligence, fuzzy logic control, maximum power point tracking (MPPT), perturb and observe (P&O), variable step-size P&O

## 1 | INTRODUCTION

The need for electrical energy for homes and industries has significantly increased in the last few decades. Many power plants have been built to meet the demand for electrical energy. However, in addition to their dwindling resources, these power plants have several adverse side effects on the environment, such as water, soil, and air pollution caused by solid and liquid waste produced from burning fossil materials as raw materials [1, 2]. However, due to the shared awareness in various circles, radical efforts have been made to overcome these problems and provide a healthier environment.

Renewable energy is one of the significant issues predicted to be the best alternative to fulfill the demand for electrical energy but without harming the environment. Renewable energy sources such as solar photovoltaic (PV) systems, hydropower, wind turbine, tidal turbine, biomass, and biothermal [3, 4] are being developed because of their ability to optimize the potential of

nature. Solar PV systems are one of the most popular because they are clean, do not cause noise, are cheap, and easy to install and maintain [5, 6]. Furthermore, the advantage of solar PV systems as an alternative power plant is that they do not generate noise compared to wind turbines [7].

However, due to the direct relationship and dependence on nature, solar PV-based power generation is nonlinear. As when the irradiation on the PV array changes drastically, at that time, an instantaneous shift in the peak power point occurs [8]. The nonlinear nature resulting from changes in irradiation and temperature affecting the PV causes the efficiency of the PV itself to be lower [9, 10]. PV energy loss has reached up to 25% [11]. This energy loss is one of the problems in optimizing energy harvesters with solar PV. Various efforts have been made to optimize energy harvesting from solar PV. One of the most effective ways to increase efficiency is to achieve solar PV power production under any conditions [12]. This technique is known as maximum power point tracking (MPPT), which works by feeding an appropriate duty cycle to DC/DC converter in the PV system.

Various methods can be used to operate MPPT, ranging from conventional methods such as perturb and observe (P&O) [13–15], incremental conductance (IncCond) [16–18], hill climbing (HC) [19–21], and their improved methods such as learning-based P&O (LPO) [22], self-tuned P&O (SPO) [23], learning-based ncCond (LIC) [24, 25], learning-based HC (L-HC) [26], which is based on the perturbation process in HC, to methods based on artificial intelligence algorithms such as fuzzy logic (FL) [27–31], artificial neural network (ANN) [32, 33], and adaptive neuro-fuzzy inference systems (ANFIS) [34–36]. Generally, a suitable MPPT implementation considers several aspects such as the type of application, efficiency, cost, lost energy, and suitability of the converter [37, 38].

There are various types of DC/DC converters developed for various applications, namely, boost, buck, and buck–boost converters. For applications that require high-voltage conversion, a DC/DC converter that can compensate for these needs is required. The boost converter can achieve high voltages by providing a large $D$. However, the voltage increment multiplication is not more than five and at the expense of efficiency, increasing the voltage on the switch and causing electromagnetic inference [39–41]. A coupled-inductor converter can provide high-voltage gain. Nevertheless, the efficiency is low due to increased chopper losses in inductors and conduction losses in semiconductors [42]. Another converter topology that provides high-gain voltage is the cascaded converter [43, 44]. However, the efficiency is also low due to the need for two processes. Another alternative is connecting two converters in series with only one switch, which is often called a quadratic boost converter (QBC) [45–47]. This converter topology produces the same voltage ratio as the cascaded converter, but the efficiency is lower than the boost converter.

The new high-gain voltage DC/DC converter [48] provides a high-voltage ratio and efficiency with lower current and voltage ripples. However, this converter still needs to be tested with MPPT to determine its suitability for PV systems. Therefore, this paper employs the FL algorithm in a high-gain voltage DC/DC converter for standalone PV systems.

## 2 | MODELING OF SOLAR CELLS

A basic understanding of solar cells is essential as a fundamental element of a PV system. Solar arrays commonly used consist of a combination of series and/or parallel PV cells to produce a specific value. Different circuit models of PV cells are presented by Jordehi [49]. As in Figure 1, the single diode is the most common and most straightforward model, whereas the PV module characteristic curves are shown in Figure 2. The relationship between the voltage–current of the PV module is modeled as

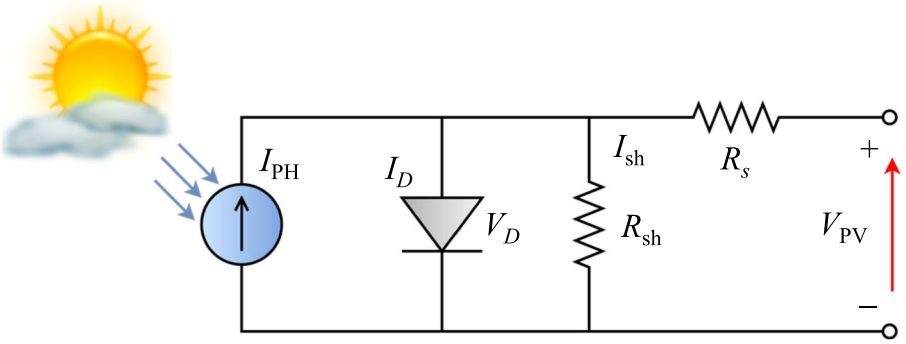


FIGURE 1 Single-diode PV model

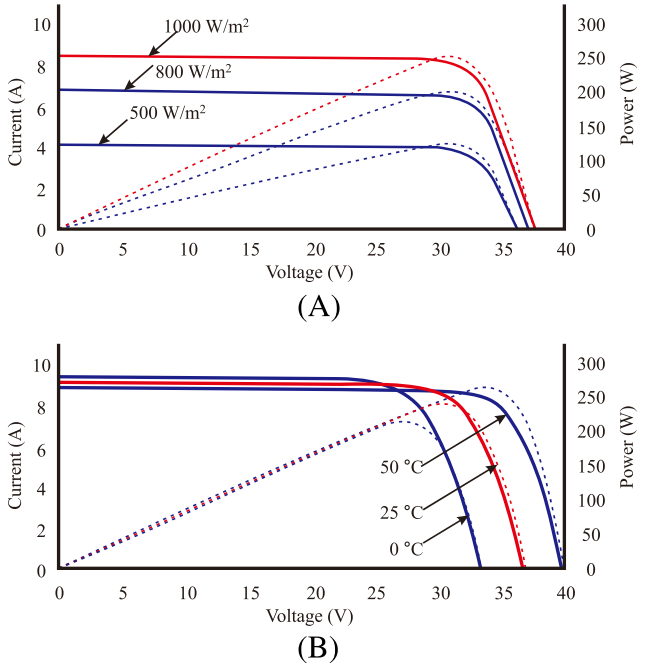


**FIGURE 2** Trina Solar TSM-250PA05.08 PV module characteristic curves (A) under irradiation variation and (B) under temperature variation

$$I = I_{PH} - I_{sat} \times \left[ \exp\left\{ q \times \frac{V_{PV} + I_{PV} \times R_S}{A \times K \times T} \right\} - 1 \right] - \frac{V_{PV} + I_{PV} \times R_S}{R_{SH}}, \quad (1)$$

where $I_{PH}$ and $I_{sat}$ are light-generated and reverse saturation current, respectively, $q$ is the electron charge ($1.66022 \times 10^{-19}$ C), $V_{PV}$ and $I_{PV}$ are the output voltage and current of the solar cells, respectively, $R_S$ and $R_{SH}$ are shunt and series resistances, respectively, $A$ is the p-n ideal factor, $K$ is the Boltzmann's constant ($1.38\times 10^{-23}$ J/K), and $T$ is the cell temperature in Kelvin.

The $I_{PH}$ value is strongly influenced by the ambient temperature, $T$, as well as the irradiance, $G$, which is expressed as

$$I_{PH} = \left\{ I_{SC}^{*} + k_i (T - T^{*}) \right\} \frac{G}{G^{*}}, \quad (2)$$

where $I_{SC}^{*}$ is the short-circuit current at 25°C, $T^{*} = 298°K$ and $G = 1000\,\mathrm{W/m^2}$. Although $k_i$ is the short-circuit current temperature coefficient. The * sign is the value at standard test conditions.

$I_{sat}$ is affected by ambient temperature as

$$I_{sat} = \frac{I_{SC}^{*} + k_i (T - T^{*})}{\exp\left[ \frac{V_{OC}^{*} + k_V (T - T^{*})}{V_t} \right] - 1}, \quad (3)$$

where $V_{OC}^{*}$ is the open-circuit voltage at 25°C with $k_V$ as the coefficient of open-circuit voltage, whereas $V_t = K \times T/q$ is the thermal voltage.

The amount of current in the series-connected module per setting is $N_{ser}$, and the parallel connection is $N_{par}$, then

$$I = N_{par} I_{PH} - N_{par} I_{sat} \left[ \exp\left\{ q \frac{\frac{V}{N_{ser}} + I \frac{R_S}{N_{par}}}{AKT} \right\} - 1 \right] - \frac{\left( \frac{N_{par}}{N_{ser}} \right) + I R_S}{R_{SH}}. \quad (4)$$

## 3 | MPPT

The maximum power transfer theorem forms the basis for the working principle of the MPPT technique. The theorem states that when the load resistance matches the source, it can transfer the maximum power. Therefore, the working principle of the MPPT technique is to ensure the load resistance with PV at the maximum power point (MPP), which is calculated by Green [50].

$$R_{mpp} = \frac{V_{mpp}}{I_{mpp}}, \quad (5)$$

where $R_{mpp}$, $V_{mpp}$, and $I_{mpp}$ are the resistance, voltage, and current in MPP, respectively.

Although the maximum power transfer can be carried out by considering $R_{mpp}$, in reality, $R_{mpp}$ is not constant because of the $I-V$ curve of PV due to weather dependence where changes in irradiation and temperature are unavoidable. Therefore, a DC/DC converter between the source and voltage connections is required to compensate for this resistance mismatch instead of supplying power directly to the load [51]. Through the MPPT algorithm, the duty cycle, $D$, is adjusted to ensure load resistance, and the $D$, which has been modified according to $R_{mpp}$ on PV under varying weather conditions.

## 4 | HIGH-GAIN VOLTAGE DC/DC CONVERTER

The DC/DC converter plays a vital role in the source and load interface of PV systems. This paper uses a high-gain

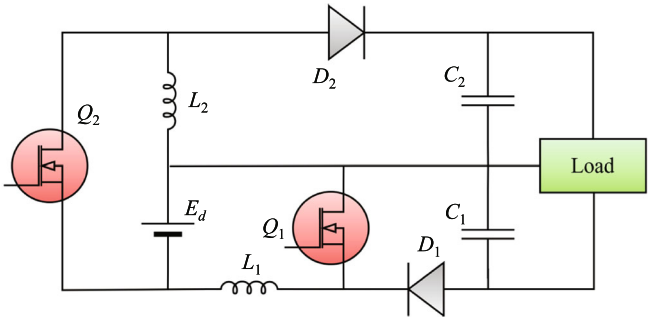


FIGURE 3 Schematic of a converter with a high-voltage ratio

voltage DC/DC converter, shown in Figure 3, based on a modified DC/DC buck–boost converter. This converter is capable of producing a high-voltage ratio obtained from

$$\frac{V_o}{E_d} = \frac{1}{1-\alpha}, \tag{6}$$

where $\alpha$ is the duty factor of the transistor $Q$.

The RMS value of the voltage ripple is given by Bahrami and others (7), whereas the output voltage ripple when the duty cycle is more than half is given by Baba and others (8).

$$\widetilde{V}_o = \frac{\bar{i}_o}{Cf_s} \frac{\alpha(1-2\alpha)}{2\sqrt{3}(1-\alpha)}, \tag{7}$$

$$\widetilde{V}_o = \frac{\bar{i}_o}{Cf_s} \frac{(2\alpha-1)}{2\sqrt{3}}, \tag{8}$$

where $f_s$ is the minimum switching of the converter.

## 5 | MPPT CONTROL ALGORITHMS

There are many variations of the MPPT control algorithm. However, one of the most frequently applied MPPT control algorithms because of its convenience is P&O. In this paper, conventional and advanced P&O algorithms based on step-size variables will be compared with one of the artificial intelligence algorithms, namely, FL.

### 5.1 | P&O

The P&O algorithm is in great demand in the MPPT technique because it does not require special information related to PV characteristics, so it can be applied to all types of PV modules [52]. Figure 4 shows a flowchart for the conventional P&O method.

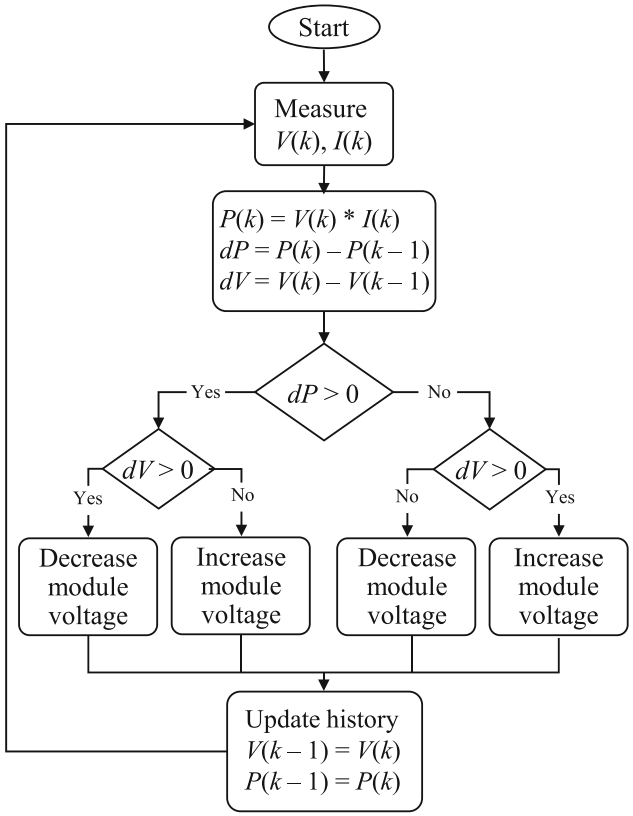


FIGURE 4 Flowchart of conventional P&O algorithm

The working principle is to direct the working point on the MPP by perturbation. If the PV operating point is to the left of the MPP, the perturbation is done to the right, and vice versa. However, this algorithm is affected by the given step size. The wide step size can speed up MPP tracking, but the oscillations around the MPP are also large. On the other hand, a small step size reduces oscillations around the MPP but slows down the tracking speed.

Adaptive P&O based on step-size variables was developed to reduce oscillations around the MPP caused by conventional P&O algorithms [53]. The flowchart of the algorithm is shown in Figure 5. In this algorithm, factor $(A)$ is used as a constant whose value is greater than 1. The duty cycle as the control output of the algorithm increases with the multiplication factor $(A)$ when $dP > 0$. Meanwhile, when the condition $dP < 0$, then the duty cycle is divided by $(A)$.

### 5.2 | FL

The FL algorithm offers advantages in the form of ease of implementation, no requirement for mathematical

modeling of data and robustness in the field of control systems [27, 54–56]. In a PV system, the input FL is the Error ($E$) resulting from the change in the PV output power divided by the change in the output voltage and the Change of Error ($\Delta E$). Although the output is the duty cycle which will regulate the PWM converter signal. Both inputs are given by.

$$\text{Error, } E(k) = \frac{\Delta P}{\Delta V} = \frac{P(k) - P(k-1)}{V(k) - V(k-1)}, \tag{9}$$

$$\text{Error Change, } \Delta E(k) = E(k) - E(k-1), \tag{10}$$

where $k$ is sample time, $P(k)$ and $V(k)$ are PV power and voltage, $P(k-1)$ and $V(k-1)$ are previous PV power and voltage.

In the fuzzification stage, a triangular subset with five membership functions is used. Additionally, symmetrical membership functions are used for input and output. Each of these membership functions is negative big (NB), negative small (NS), zero (Z), positive small (PS), and positive big (PB). The knowledge based on the Mamdani-type inference system process is shown in Table 1, whereas the results of the rule base are depicted by the surface Figure 6. Thus, in the defuzzification process, the center of gravity method is used.

## 6 | RESULTS AND DISCUSSION

In this paper, the Trina Solar TSM-250PA05.08 PV module with the parameters as described in Table 2 is used. The characteristics of the PV output that are affected by irradiance and ambient temperature are shown in Figure 2. The proposed system is constructed in MATLAB/Simulink for a standalone application with a resistive load, which is comprehensively shown in Figure 7.

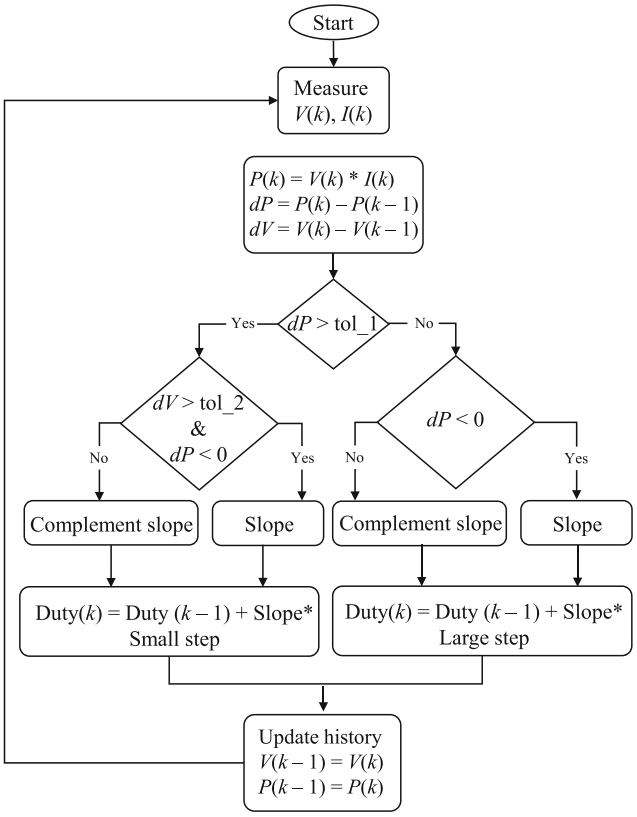


FIGURE 5 Flowchart of P&O variable step-size algorithm

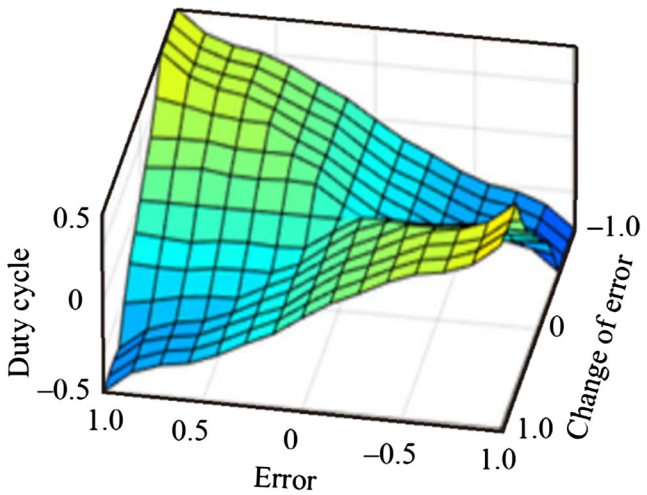


FIGURE 6 Surface inference system stage

TABLE 1 Knowledge base

| E/ΔE | Negative big (NB) | Negative small (NS) | Zero (Z) | Positive small (PS) | Positive big (PB) |
|---|---|---|---|---|---|
| Negative big (NB) | NB | NB | Z | PB | PB |
| Negative small (NS) | NS | NS | Z | PS | PS |
| Zero (Z) | Z | Z | Z | Z | Z |
| Positive small (PS) | PS | PS | Z | NS | NS |
| Positive big (Pb) | PB | PB | Z | NB | NB |

System testing is done by varying the irradiance into six steps. The irradiance variations given in the sequence of steps 1–6 are 1000, 700, 800, 600, 400, and 200 W/m$^2$. This test was conducted to determine the agility of the MPPT algorithm employed in high-gain voltage converters with varying weather conditions. Figure 8 shows the results of testing the FL algorithm on the MPPT technique when handling variations of simulated weather conditions by varying the irradiance. The FL algorithm was compared with conventional P&O and variable step-size P&O as described.

**TABLE 2** Trina Solar TSM-250PA05.08 PV module characteristics

| Parameters | Value |
|---|---|
| Maximum power, $P_{MPP}$ | 249.86 (W) |
| Cells per module, $N_{cell}$ | 60 cells |
| Open-circuit voltage, $V_{OC}$ | 37.6 (V) |
| Short-circuit current, $I_{SC}$ | 8.55 (A) |
| Voltage at maximum power point, $V_{MP}$ | 31 (V) |
| Current at maximum power point, $I_{MP}$ | 8.06 (A) |
| Temperature coefficient of $V_{OC}$ | −0.35%/°C |
| Temperature coefficient of $I_{SC}$ | 0.06%/°C |

As shown in Figure 8, conventional P&O and variable step-size P&O experience an overshoot of the curve. This phenomenon is known as drift, which is caused by a misjudgment of the MPPT algorithm so that the operating point will deviate from the true MPP [57, 58]. Drift is common in algorithms with operations based on hill climbing, such as P&O, which experience sudden changes in irradiation. In this test, drift also occurs in the step-size P&O variable, but it is not as severe as in conventional P&O.

It is different from the FL algorithm, which does not experience the drift phenomenon at all. The FL algorithm is able to operate the MPPT technique on a high-gain voltage converter properly. Besides not experiencing drift, the FL algorithm is also able to track MPP quickly. This is proven by the tracking speed, which is better than the P&O algorithm. It can be seen in Figure 9 that the curve generated by the FL algorithm is more stable than P&O, especially without the step-size variable. When the system is first subjected to high irradiation treatment (Figure 9A), both conventional P&O and variable step-size P&O oscillate around the MPP until they are finally able to track the true MPP. The process to the actual MPP after this oscillation takes time, causing losses in the system. Likewise, when given low irradiation treatment, the two P&O algorithms drifted, causing the

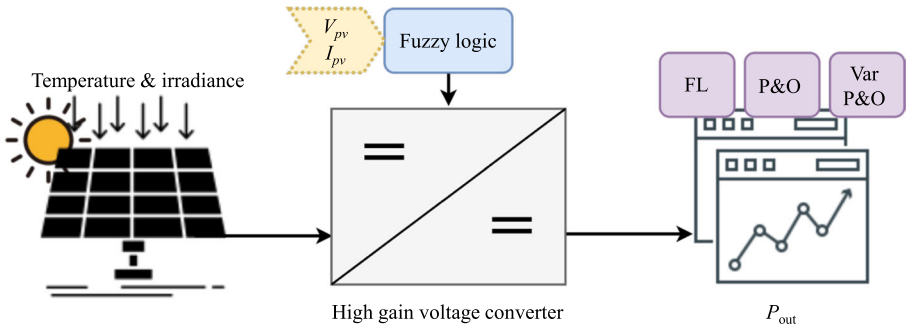


**FIGURE 7** The proposed system simulated with MATLAB/Simulink

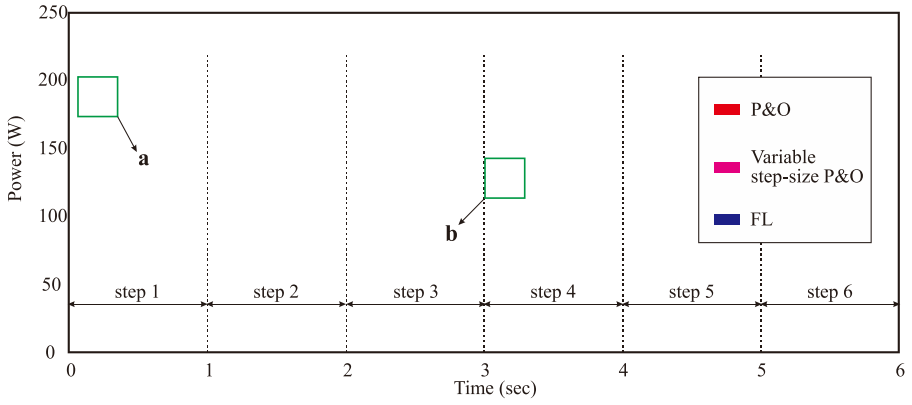


**FIGURE 8** $P_{out}$ generated by given the variation of irradiance

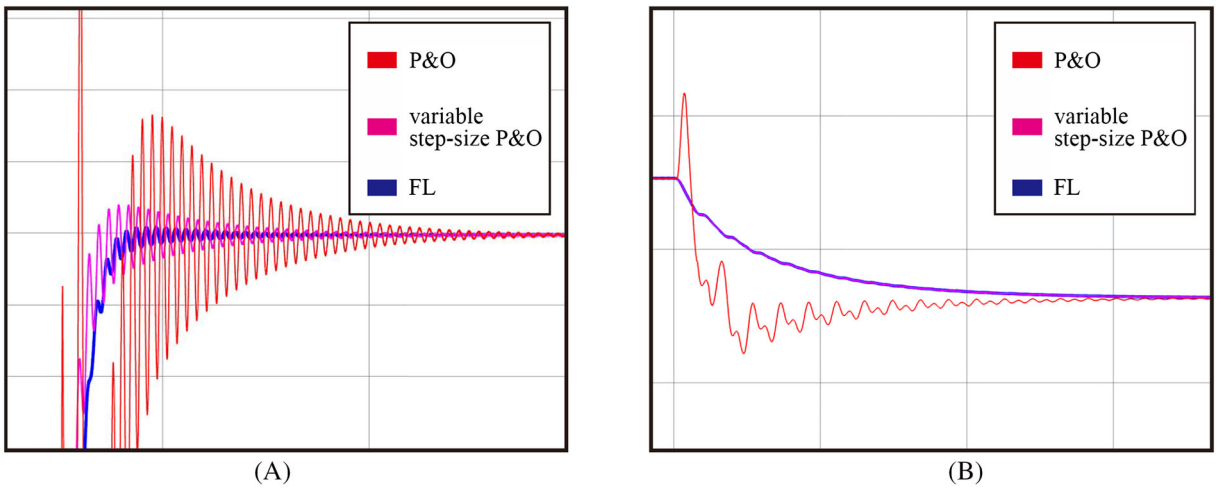


**FIGURE 9** Details of drift and initial oscillation of $P_{out}$ (A) when the irradiation level increases and (B) when the irradiation level decreases

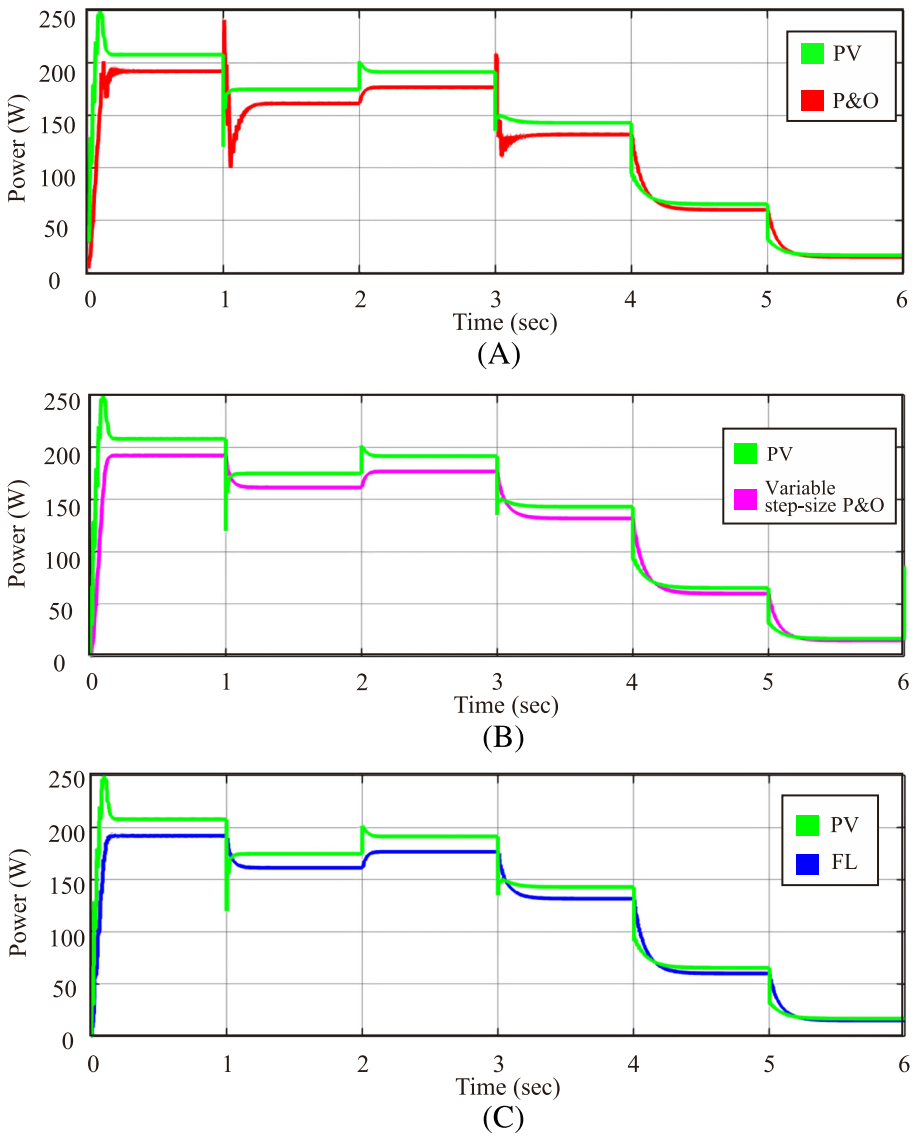


**FIGURE 10** Comparison of $P_{out}$ PV against (A) conventional P&O, (B) variable step-size P&O, and (C) FL

system to be unresponsive. These two disadvantages do not occur in the FL algorithm.

Furthermore, several parameters affecting the performance of the MPPT system were carefully examined from the three algorithms. These parameters are tracking speed, oscillation, and efficiency. Overall, the FL algorithm can track MPP faster, namely, 0.25 s, followed by the step-size P&O variable with a tracking time of 0.41 s. At the same time, conventional P&O can only track MPP after 0.52 s. The oscillations around MPP caused by the FL algorithm are also quite small (0.01 V), whereas the step-size and conventional P&O variables are 0.86 and 1.22 V, respectively.

However, the efficiency generated by the three algorithms has the same level of 93.66%. Figure 10 shows the comparison of $P_{out}$ PV against the three MPPT algorithms. Seen in Figure 10A, the P&O algorithm reacts to an extreme when there is a change in irradiation. The P&O algorithm causes an instantaneous drift when the irradiation changes and takes longer to return to a stable state. Different results are shown in the FL algorithm and the step-size P&O variable, where there is no extreme reaction when irradiation changes. Both tend to produce a smoother slope. Also, when viewed in more detail, as shown in Figure 9A, the step-size P&O algorithm tends to have oscillations even though they only look small.

The FL algorithm can track MPP quickly because it does not go through a subtraction and addition process as the P&O algorithm does. Although the variable step-size P&O can provide large step perturbations away from MPP, it still needs to track MPP as fast as the FL algorithm. Furthermore, the oscillations caused by P&O are more significant. The perturbation step length causes large oscillations around the MPP. In the conventional P&O algorithm that uses a fixed step size, the magnitude of the oscillation is the same as the step size used. This paradigm of problems occurs in conventional P&O algorithms, where a wide step size can shorten the MPPT tracking process, but the oscillations around the MPP become large. On the other hand, a small step size will minimize oscillations, but it will take longer to reach MPP.

In terms of efficiency, the three algorithms do not affect the power harvesting efficiency of the high-gain DC/DC converter used. All three algorithms can actually be applied to the new converter topology. However, the FL algorithm is able to outperform conventional and variable step-size P&O algorithms in terms of tracking speed and oscillation damping.

## 7 | CONCLUSION

MPPT control with a new topology converter that has never been tested on MPPT PV system techniques has been completed. MPPT is operated using the FL algorithm as one of the various types of intelligent algorithms. MPPT performance with this FL algorithm is compared with the P&O algorithm as the most commonly used algorithm and adaptive P&O, which is based on step-size variables as the development of the P&O algorithm. The test is performed by varying the irradiance to represent weather changes around the PV module. The results indicate that the FL algorithm can outperform conventional P&O algorithms and step-size variables. This is evidenced by the faster tracking speed and smaller oscillations generated by the FL algorithm. The P&O algorithm reacts to extremes when there is a change in irradiation, which causes a momentary deviation when the irradiation changes and takes longer to return to a stable state. However, the FL algorithm shows no extreme reaction when the irradiation changes. Therefore, the MPPT technique becomes more convergent, and the MPP is ensured to be tracked correctly by the FL algorithm. This advantage makes solar energy harvesting through the PV system with the MPPT technique, which is operated by the FL algorithm, more optimum.

## CONFLICT OF INTEREST

The authors declare that there are no conflicts of interest.

## ORCID

*Arsyad Cahya Subrata* https://orcid.org/0000-0002-7336-2884

## REFERENCES

1. L. Xiaoping, Q. Yunyou, and S. SaeidNahaei, *A novel maximum power point tracking in partially shaded PV systems using a hybrid method*, Int. J. Hydrogen Energy **46** (2021), 37351–37366.
2. I. Dincer, *Renewable energy and sustainable development: A crucial review*, Renew. Sustain. Energy Rev. **4** (2000), 157–175.
3. A. Chatterjee, K. Mohanty, V. S. Kommukuri, and K. Thakre, *Design and experimental investigation of digital model predictive current controller for single phase grid integrated photovoltaic systems*, Renew. Energy **108** (2017), 438–448.
4. R. Gross, M. Leach, and A. Bauen, *Progress in renewable energy*, Environ. Int. **29** (2003), 105–122.
5. M. AlShabi, C. Ghenai, M. Bettayeb, and F. F. Ahmad, *Estimating one-diode-PV model using autonomous groups particle swarm optimization*, IAES Int. J. Artif. Intell. **10** (2021), no. 1, 166–174.
6. M. AlShabi, C. Ghenai, M. Bettayeb, F. F. Ahmad and M. El Haj Assad, *Estimating pv models using multi-group salp swarm algorithm*, IAES Int. J. Artif. Intell. **10** (2021), no. 2, 398–406.
7. M. Bahrami, R. Gavagsaz-Ghoachani, M. Zandi, M. Phattanasak, G. Maranzanaa, B. Nahid-Mobarakeh, S. Pierfederici, and F. Meibody-Tabar, *Hybrid maximum power point tracking algorithm with improved dynamic performance*, Renew. Energy **130** (2019), 982–991.

8. A. O. Baba, G. Liu, and X. Chen, *Classification and evaluation review of maximum power point tracking methods*, Sustain. Futur. **2** (2020), 100020.
9. S. Dubey, J. N. Sarvaiya, and B. Seshadri, *Temperature dependent photovoltaic (PV) efficiency and its effect on PV production in the world–a review*, Energy Procedia **33** (2013), 311–321.
10. A. A. Abdulrazzaq and A. H. Ali, *Efficiency performances of two MPPT algorithms for PV system with different solar panels irradiances*, Int. J. Power Electron. Drive Syst. **9** (2018), no. 4, 1755–1764.
11. E. Roman, R. Alonso, P. Ibanez, S. Elorduizapatarietxe, and D. Goitia, *Intelligent PV module for grid-connected PV systems*, IEEE Trans. Ind. Electron. **53** (2006), 1066–1073.
12. S. D. Al-Majidi, M. F. Abbod, and H. S. Al-Raweshidy, *A novel maximum power point tracking technique based on fuzzy logic for photovoltaic systems*, Int. J. Hydrogen Energy **43** (2018), 14158–14171.
13. J. Ahmed and Z. Salam, *An enhanced adaptive P&O MPPT for fast and efficient tracking under varying environmental conditions*, IEEE Trans. Sustain. Energy **9** (2018), 1487–1496.
14. A.-R. Youssef, H. H. H. Mousa, and E. E. M. Mohamed, *Development of self-adaptive P&O MPPT algorithm for wind generation systems with concentrated search area*, Renew. Energy **154** (2020), 875–893.
15. M. Abdel-Salam, M. T. El-Mohandes, and M. El-Ghazaly, *An efficient tracking of MPP in PV systems using a newly-formulated P&O-MPPT method under varying irradiation levels*, J. Electr. Eng. Technol. **15** (2020), 501–513.
16. M. N. Ali, K. Mahmoud, M. Lehtonen, and M. M. F. Darwish, *An efficient fuzzy-logic based variable-step incremental conductance MPPT method for grid-connected PV systems*, IEEE Access **9** (2021), 26420–26430.
17. A. K. Gupta, R. K. Pachauri, T. Maity, Y. K. Chauhan, O. P. Mahela, B. Khan, and P. K. Gupta, *Effect of various incremental conductance MPPT methods on the charging of battery load feed by solar panel*, IEEE Access **9** (2021), 90977–90988.
18. H. Shahid, M. Kamran, Z. Mehmood, M. Y. Saleem, M. Mudassar, and K. Haider, *Implementation of the novel temperature controller and incremental conductance MPPT algorithm for indoor photovoltaic system*, Sol. Energy **163** (2018), 235–242.
19. V. Jately, B. Azzopardi, J. Joshi, A. Sharma, and S. Arora, *Experimental analysis of hill-climbing MPPT algorithms under low irradiance levels*, Renew. Sustain. Energy Rev. **150** (2021), 111467.
20. W. Zhu, L. Shang, P. Li, and H. Guo, *Modified hill climbing MPPT algorithm with reduced steady-state oscillation and improved tracking efficiency*, J. Eng. **2018** (2018), 1878–1883.
21. C. B. N. Fapi, P. Wira, M. Kamta, A. Badji, and H. Tchakounte, *Real-time experimental assessment of hill climbing MPPT algorithm enhanced by estimating a duty cycle for PV system*, Int. J. Renew. Energy Res. **9** (2019), no. 3, 1180–1189.
22. N. Kumar, B. Singh, and B. K. Panigrahi, *LLMLF-based control approach and LPO MPPT technique for improving performance of a multifunctional three-phase two-stage grid integrated PV system*, IEEE Trans. Sustain. Energy **11** (2019), 371–380.
23. N. Kumar, B. Singh, and B. K. Panigrahi, *Integration of solar PV with low-voltage weak grid system: Using maximize-M Kalman filter and self-tuned P&O algorithm*, IEEE Trans. Ind. Electron. **66** (2019), 9013–9022.
24. N. Kumar, B. Singh, B. K. Panigrahi, and L. Xu, *Leaky-least-logarithmic-absolute-difference-based control algorithm and learning-based InC MPPT technique for grid-integrated PV system*, IEEE Trans. Ind. Electron. **66** (2019), 9003–9012.
25. N. Kumar, B. Singh, B. K. Panigrahi, C. Chakraborty, H. M. Suryawanshi, and V. Verma, *Integration of solar PV with low-voltage weak grid system: Using normalized laplacian kernel adaptive kalman filter and learning based InC algorithm*, IEEE Trans. Power Electron. **34** (2019), 10746–10758.
26. N. Kumar, B. Singh, J. Wang, and B. K. Panigrahi, *A framework of L-HC and AM-MKF for accurate harmonic supportive control schemes*, IEEE Trans. Circuits Syst. I Regul. Pap. **67** (2020), 5246–5256.
27. H. Rezk, M. Aly, M. Al-Dhaifallah, and M. Shoyama, *Design and hardware implementation of new adaptive fuzzy logic-based MPPT control method for photovoltaic applications*, IEEE Access **7** (2019), 106427–106438.
28. S. Farajdadian and S. M. H. Hosseini, *Optimization of fuzzy-based MPPT controller via metaheuristic techniques for standalone PV systems*, Int. J. Hydrogen Energy **44** (2019), 25457–25472.
29. X. Li, H. Wen, Y. Hu, and L. Jiang, *A novel beta parameter based fuzzy-logic controller for photovoltaic MPPT application*, Renew. Energy **130** (2019), 416–427.
30. U. Yilmaz, A. Kircay, and S. Borekci, *PV system fuzzy logic MPPT method and PI control as a charge controller*, Renew. Sustain. Energy Rev. **81** (2018), 994–1001.
31. X. Ge, F. W. Ahmed, A. Rezvani, N. Aljojo, S. Samad, and L. K. Foong, *Implementation of a novel hybrid BAT-fuzzy controller based MPPT for grid-connected PV-battery system*, Control Eng. Pract. **98** (2020), 104380.
32. R. B. Roy, M. Rokonuzzaman, N. Amin, M. K. Mishu, S. Alahakoon, S. Rahman, N. Mithulananthan, K. S. Rahman, M. Shakeri, and J. Pasupuleti, *A comparative performance analysis of ANN algorithms for MPPT energy harvesting in solar PV system*, IEEE Access **9** (2021), 102137–102152.
33. B. Babes, A. Boutaghane, and N. Hamouda, *A novel nature-inspired maximum power point tracking (MPPT) controller based on ACO-ANN algorithm for photovoltaic (PV) system fed arc welding machines*, Neural Comput. Applic. **34** (2022), 299–317.
34. K. J. Reddy and N. Sudhakar, *ANFIS-MPPT control algorithm for a PEMFC system used in electric vehicle applications*, Int. J. Hydrogen Energy **44** (2019), 15355–15369.
35. K. Amara, A. Fekik, D. Hocine, M. L. Bakir, E. -B. Bourennane, T. A. Malek, and A. Malek, *Improved performance of a PV solar panel with adaptive neuro fuzzy inference system ANFIS based MPPT*, (2018 7th International Conference on Renewable Energy Research and Applications (ICRERA), Paris, France), 2018, pp. 1098–1101.
36. A. A. Aldair, A. A. Obed, and A. F. Halihal, *Design and implementation of ANFIS-reference model controller based MPPT using FPGA for photovoltaic system*, Renew. Sustain. Energy Rev. **82** (2018), 2202–2217.
37. M. Birane, C. Larbes, and A. Cheknane, *Comparative study and performance evaluation of central and distributed*

*topologies of photovoltaic system*, Int. J. Hydrogen Energy **42** (2017), 8703–8711.
38. Z. Salam, J. Ahmed, and B. S. Merugu, *The application of soft computing methods for MPPT of PV system: A technological and status review*, Appl. Energy **107** (2013), 135–148.
39. S. Ozdemir, N. Altin, and I. Sefa, *Fuzzy logic based MPPT controller for high conversion ratio quadratic boost converter*, Int. J. Hydrogen Energy **42** (2017), 17748–17759.
40. N. Zhang, D. Sutanto, K. M. Muttaqi, B. Zhang, and D. Qiu, *High-voltage-gain quadratic boost converter with voltage multiplier*, IET Power Electron. **8** (2015), 2511–2519.
41. P. Saadat and K. Abbaszadeh, *A single-switch high step-up DC–DC converter based on quadratic boost*, IEEE Trans. Ind. Electron. **63** (2016), 7733–7742.
42. A. C. Subrata, T. Sutikno, S. Padmanaban, and H. S. Purnama, Maximum power point tracking in pv arrays with high gain DC-DC boost converter, in International Conference on Electrical Engineering, Computer Science and Informatics (EECSI), 2019.
43. X. Zhang, Y. Hu, W. Mao, T. Zhao, M. Wang, F. Liu, and R. Cao, *A grid-supporting strategy for cascaded H-bridge PV converter using VSG algorithm with modular active power reserve*, IEEE Trans. Ind. Electron. **68** (2020), 186–197.
44. Y. Pan, A. Sangwongwanich, Y. Yang, and F. Blaabjerg, *A phase-shifting MPPT to mitigate interharmonics from cascaded H-bridge PV inverters*, IEEE Trans. Ind. Appl. **57** (2020), 3052–3063.
45. S. Srinivasan, R. Tiwari, M. Krishnamoorthy, M. P. Lalitha, and K. K. Raj, *Neural network based MPPT control with reconfigured quadratic boost converter for fuel cell application*, Int. J. Hydrogen Energy **46** (2021), 6709–6719.
46. K. Kumar, S. R. Kiran, T. Ramji, S. Saravanan, P. Pandiyan, and N. Prabaharan, *Performance evaluation of photo voltaic system with quadratic boost converter employing with MPPT control algorithms*, Int. J. Renew. Energy Res. **10** (2020), 1083–1091.
47. S. K. Manas and B. Bhushan, *Performance Analysis of Fuzzy Logic-Based MPPT Controller for Solar PV System Using Quadratic Boost Converter*, In *Advances in energy technology*, Springer, 2022, 69–79.
48. P. A. Dahono, *Derivation of high voltage-gain step-up DC-DC power converters*, Int. J. Electr. Eng. Informatics **11** (2019).
49. A. R. Jordehi, *Parameter estimation of solar photovoltaic (PV) cells: A review*, Renew. Sustain. Energy Rev. **61** (2016), 354–371.
50. M. A. Green, *Accuracy of analytical expressions for solar cell fill factors*, Sol. Cells **7** (1982), 337–340.
51. M. G. Batarseh and M. E. Za'ter, *Hybrid maximum power point tracking techniques: A comparative survey, suggested classification and uninvestigated combinations*, Sol. Energy **169** (2018), 535–555.
52. J. Kivimäki, S. Kolesnik, M. Sitbon, T. Suntio, and A. Kuperman, *Design guidelines for multiloop perturbative maximum power point tracking algorithms*, IEEE Trans. Power Electron. **33** (2017), 1284–1293.
53. A. Bin Jusoh, O. J. E. I. Mohammed, and T. Sutikno, *Variable step size perturb and observe MPPT for PV solar applications*, Telkomnika **13** (2015), 1.
54. D. N. Luta and A. K. Raji, *Comparing fuzzy rule-based MPPT techniques for fuel cell stack applications*, Energy Procedia **156** (2019), 177–182.
55. S. Assahout, H. Elaissaoui, A. El Ougli, B. Tidhaf, and H. Zrouri, *A neural network and fuzzy logic based MPPT algorithm for photovoltaic pumping system*, Int. J. Power Electron. Drive Syst. **9** (2018), 1823–1833.
56. T. Sutikno, A. C. Subrata, and A. Elkhateb, *Evaluation of fuzzy membership function effects for maximum power point tracking technique of photovoltaic system*, IEEE Access **9** (2021), 109157–109165.
57. M. Killi and S. Samanta, *Modified perturb and observe MPPT algorithm for drift avoidance in photovoltaic systems*, IEEE Trans. Ind. Electron. **62** (2015), 5549–5559.
58. X. Li, H. Wen, Y. Hu, and L. Jiang, *Drift-free current sensorless MPPT algorithm in photovoltaic systems*, Sol. Energy **177** (2019), 118–126.

## AUTHOR BIOGRAPHIES

**Sunardi Sangsang Sasmowiyono** received his B.E. and M.E. in Electrical Engineering from Universitas Gadjah Mada and Institut Teknologi Bandung in 1999 and 2003, respectively. He also received his Ph.D. degree in Electrical Engineering from Universiti Teknologi Malaysia in 2011. He is currently working as an Associate Professor with the Electrical Engineering Department, Universitas Ahmad Dahlan (UAD), Yogyakarta, Indonesia. His current research interests include signal processing, image processing, and artificial intelligence. He can be contacted at email: sunardi@mti.uad.ac.id.

**Abdul Fadlil** received his B.E. in Physics—Electronics and Instrumentation and M.E. in Electrical Engineering from Universitas Gadjah Mada in 1992 and 2000, respectively. He also received his Ph.D. degree in Electrical Engineering from Universiti Teknologi Malaysia in 2006. He is currently as Associate Professor with the Electrical Engineering Department, Universitas Ahmad Dahlan (UAD), Yogyakarta, Indonesia. His current research interests include pattern recognition, image processing, and artificial intelligence. He can be contacted at email: fadlil@mti.uad.ac.id.

**Arsyad Cahya Subrata** received his B.E. and M.E. in Electrical Engineering from Universitas Ahmad Dahlan, Indonesia, and Universitas Diponegoro, Indonesia, in 2016 and 2020, respectively. He has been the Head of Technology at a start-up company engaged in automation in agriculture-livestock, health, aerial monitoring, and industrial automation since 2017. Currently, he is a member of the Embedded Systems and Power Electronics Research Group (ESPERG) research team since 2018 and has been a Lecturer with the Electrical Engineering Department, Universitas Ahmad Dahlan (UAD), Yogyakarta, Indonesia, since 2021. His research interests include renewable energy, robotics, artificial intelligence, control instrumentation, intelligent control, and Internet of Things. He can be contacted at email: arsyad.subrata@te.uad.ac.id.

**How to cite this article:** S. Sangsang Sasmowiyono, A. Fadlil, and A. C. Subrata, *Optimum solar energy harvesting system using artificial intelligence*, ETRI Journal **45** (2023), 996–1006. DOI 10.4218/etrij.2022-0184